

# Wavelength-tuning interferometry of intraocular distances

F. Lexer, C. K. Hitzenberger, A. F. Fercher, and M. Kulhavy

We describe basic principles of wavelength-tuning interferometry and demonstrate its application in ophthalmology. The advantage of this technique compared with conventional low-coherence interferometry ranging is the simultaneous measurement of the object structure without the need for a moving reference mirror. Shifting the wavelength of an external-cavity tunable laser diode causes intensity oscillations in the interference pattern of light beams remitted from the intraocular structure. A Fourier transform of the corresponding wave-number-dependent photodetector signal yields the distribution of the scattering potential along the light beam illuminating the eye. We use an external interferometer to linearize the wave-number axis. We obtain high resolution in a model eye by slow tuning over a wide wavelength range. With lower resolution we demonstrate the simultaneous measurement of anterior segment length, vitreous chamber depth, and axial eye length in human eyes *in vivo* with data-acquisition times in the millisecond range. © 1997 Optical Society of America

*Key words:* Wavelength tuning, interferometry, wavelength-tuning interferometry, intraocular distances.

## 1. Introduction

The precise knowledge of intraocular distances is in increasing demand in modern ophthalmology. One needs the axial eye length and the anterior chamber depth to calculate the refractive power of artificial intraocular lenses for cataract surgery. Precise measurement of the corneal thickness is essential for corneal refractive surgery, and the determination of the thickness of retinal layers might improve the diagnosis of several diseases and be helpful in monitoring therapeutic effects. In recent years a new noncontact technique, partial coherence interferometry (PCI), has been developed. PCI enables the measurement of intraocular distances with unprecedented precision and resolution.<sup>1-3</sup> This technique was extended to optical coherence tomography (OCT), a new imaging modality capable of obtaining two-dimensional optical cross sections of ocular structures.<sup>4-6</sup> Both techniques work in the time domain. A broadband light source such as a superluminescent diode is coupled with a Michelson interferometer. The sample to be measured is

placed in one arm of the interferometer; the other arm contains the reference mirror. The reference path length is changed in order to match the light transit times in the reference beam to the light transit time in the object.

An alternative approach for measuring optical distances is to use frequency- or Fourier-domain techniques. In these techniques a fixed-reference path length is used. The object is illuminated by a broadband light source, and the frequency- or wave-number-dependent response of the object on the remitted light is detected with a photodetector-array spectrometer or by tuning the wavelength.<sup>7</sup> Spectrometric techniques have already been used to measure the anomalous dispersion of gases and metal vapors,<sup>8,9</sup> the thickness and refractive index of laminae,<sup>10,11</sup> the film thickness of semiconductor layers,<sup>12</sup> the absolute displacements,<sup>13</sup> and recently the group delay on laser mirrors.<sup>14</sup> The distance information is contained in the width of channels in the spectrum. In addition, the application of spectrometric techniques used to measure single<sup>7,15</sup> and multiple intraocular distances<sup>16-18</sup> have been described.

In wavelength-tuning interferometry (WTI) the object is illuminated by a tunable laser at different wavelengths. In this case one can record the spectrum with a single photodetector. A simplified version of this technique has already been used to measure the axial length of human eyes. The distance information was obtained by counting the in-

---

The authors are with the Institute of Medical Physics, University of Vienna, Währinger Strasse 13, A-1090 Wien, Austria.

Received 2 December 1996; revised manuscript received 26 February 1997.

0003-6935/97/256548-06\$10.00/0

© 1997 Optical Society of America

interference fringes that pass a fixed point in an interferogram while the wavelength of a pulse-mode-operated laser diode was changed.<sup>19</sup> However, this fringe-counting method does not exploit the full information content of the time-domain signal and can therefore only be used if a single distance is to be measured. To obtain access to more complex object structures, one can use backscattering techniques.<sup>18</sup> WTI has some previous history: In 1960, Hymans *et al.*<sup>20</sup> described a radar system with a sawtooth frequency sweep. Later fiber-optic frequency-domain reflectometry techniques were described by MacDonald<sup>21</sup> by using a rf-modulated laser beam and Eickhoff and Ulrich<sup>22</sup> by using frequency tuning of a He-Ne laser. Currently, the most promising coherent tunable light sources are semiconductor lasers and solid-state lasers. To achieve laser tuning, the gain margins of the cavity modes have to be rearranged or the frequency of the cavity modes must be shifted. Several techniques such as distributed Bragg reflector lasers, multisection distributed feedback lasers, multiple-cavity lasers, external-cavity lasers, and filter techniques<sup>23</sup> have been developed.<sup>24</sup> To exploit the full potential of WTI, it is important that wavelength tuning is performed continuously without nonlinearities and jumps as caused by mode hops.

We present an improvement of WTI that can measure several intraocular distances simultaneously. We use an external-cavity laser. However, other continuously tunable transversal single-mode lasers might be used within their mode-hop-free spectral range. We demonstrate the WTI technique in a model eye with high resolution and in human eyes *in vivo* with low resolution but an acquisition time in the millisecond range.

## 2. Fourier-Domain Backscattering Optical Coherence Tomography

If an object is illuminated by a monochromatic wave with wavelength  $\lambda$  and wave vector  $\mathbf{k}_i$ , the Fourier transform of the diffracted homogeneous wave immediately outside the object is related to the Fourier transform of the object scattering potential along a semicircular arc in Fourier ( $\mathbf{K}$ -) space.<sup>25</sup>  $\mathbf{k}_s$  is the wave vector of the scattered wave;  $|\mathbf{k}_i| = |\mathbf{k}_s| = 2\pi/\lambda$ .  $\mathbf{K} = \mathbf{k}_s - \mathbf{k}_i$  is the scattering vector. This forms the basis of the Fourier diffraction theorem.<sup>26</sup> Furthermore, the scattered wave detected in the far field  $E^{(s)}(\mathbf{k}_s)$  is directly related to the Fourier transform of the object<sup>18,27</sup>:

$$\begin{aligned} E^{(s)}(\mathbf{k}_s) &\propto \int F(\mathbf{r}) \exp(-i \cdot \mathbf{K} \cdot \mathbf{r}) \cdot d^3\mathbf{r} \\ &= FT\{F(\mathbf{r})\} = \tilde{F}(\mathbf{K}). \end{aligned} \quad (1)$$

$F(\mathbf{r}) = -k^2[m^2(\mathbf{r}) - 1]$  is the scattering potential of the object, and  $m = n + ik$  is the object's complex refractive index. If the scattered light wave is detected at various scattering angles  $\theta$ , Fourier data of the object structure can be collected at the surface of

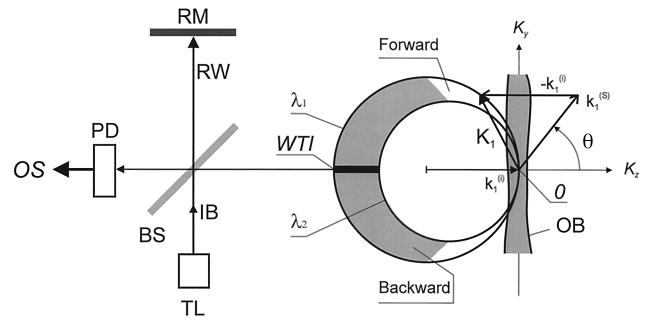


Fig. 1. Fourier space representation of forward and backward scattering: O, origin of the scattering geometry; OS, object signal; TL, tunable laser; IB, illuminating light beam; BS, beam splitter; OB, object; PD, photodetector; RM, reference mirror; RW, reference wave. Shown are the Ewald spheres corresponding to wavelengths  $\lambda_1$  and  $\lambda_2$  and the Fourier data spaces available by forward and backward scattering. WTI is the Fourier data range used by wavelength-tuning interferometry.

the so-called Ewald sphere.<sup>28</sup> When one uses a wavelength range from  $\lambda_1$  to  $\lambda_2$ , Fourier data in a volume between the corresponding Ewald spheres are available, as indicated in Fig. 1. Basically, as Fig. 1 shows, only high spatial frequency components, i.e., discontinuities in the scattering potential, can be detected with backscattered light.<sup>29,30</sup>

Though the object structure  $F(\mathbf{r})$  could readily be obtained from the scattered field data  $E^{(s)}(\mathbf{k}_s)$  by a straightforward Fourier inversion,<sup>27</sup> this technique has not been used in OCT so far. To obtain a high-resolution, two-dimensional tomogram with, e.g.,  $N^2 = 10^6$  pixel, this technique would require  $N^{3/2} = 10^9$  three-dimensional Fourier data detected with the help of a photodetector array, which to the best of our knowledge is beyond available array technology. Several modifications of this straightforward technique, however, are possible and discussed elsewhere.<sup>31</sup>

In WTI only a point detector is used, the wavelength is tuned from  $\lambda_1$  to  $\lambda_2$ , and  $\tilde{F}(\mathbf{K})$  is obtained.<sup>18</sup> In backscattering WTI the photodetector is positioned at  $\theta = \pi$  (see Fig. 1). Hence there is access only to Fourier data  $\tilde{F}(0, 0, K_z)$  along the  $K_z$  axis. There is no transversal resolution but only access to depth information. From Eq. (1) we have

$$\begin{aligned} FT^{-1}\{\tilde{F}(0, 0, K_z)\} &= FT^{-1}\{E^{(s)}[0, 0, k_z^{(s)}]\} \\ &= \iint F(x, y, z) dx dy \equiv P(z); \end{aligned} \quad (2)$$

i.e.,  $E^{(s)}$  equals the Fourier transform of the projection  $P(z)$  of the object scattering potential normal to the illuminating wave vector. Hence the transversal resolution of this technique is given by the width of the illuminating light beam. One can estimate the depth resolution with the Fourier uncertainty principle. Usually this principle is expressed in terms of the variances of the squared Fourier-transform pairs.<sup>32</sup> In optics, however, the product of the full widths at half-maximum of the Fourier-transform

pairs is more useful and for Gaussian functions leads to

$$\Delta z \Delta K_z = 8 \ln 2,$$

yielding a depth resolution of

$$\Delta z = \frac{2 \ln 2}{\pi} \frac{\lambda^2}{\Delta \lambda}. \quad (3)$$

### 3. Backscattered Light Field Measurement

In backscattering OCT one can measure the wave scattered by the object in the negative  $z$  direction. No other scattering direction is considered; hence we can simplify the notation  $E^{(O)}[0, 0, k_z^{(s)}] \equiv E^{(O)}(k)$ ;  $k$  is the wave number of the light used. This wave is superimposed onto a reference wave  $E^{(R)}$  at the photodetector, yielding the intensity  $I(k)$ :

$$\begin{aligned} I(k) &= |E^{(R)}(k) + E^{(O)}(k)|^2 \\ &= |E^{(R)}(k)|^2 + |E^{(O)}(k)|^2 + 2|E^{(R)}(k)||E^{(O)}(k)| \\ &\quad \times \cos[\phi^{(O)}(k) + \Delta\Phi(k)], \end{aligned} \quad (4)$$

where  $\phi^{(O)}$  is the phase of  $E^{(O)}$  and  $\Delta\Phi$  is the phase difference corresponding to the interferometer path difference  $d$  between the origin  $O$  of the scattering geometry and the reference mirror  $RM$  (Fig. 1):

$$\Delta\Phi = 4\pi(d/\lambda). \quad (5)$$

Usually the reference wave intensity is chosen to be constant and stronger than the object wave intensity. Then  $I(k)$  can be approximated by

$$I(k) \approx C_1 + C_2|E^{(O)}(k)|\cos[\phi^{(O)}(k) + \Delta\Phi(k)], \quad (6)$$

with  $C_1$  and  $C_2$  being constants.

In WTI the  $k$  dependence of  $I(k)$  is converted into a time dependence by tuning the wave number  $k$  of the illuminating wave with a constant wave-number rate  $\dot{k} = dk/dt$ . If  $\Delta\Phi \gg \phi^{(O)}$ , this leads to a harmonic modulation of  $I(k)$  with a (time) frequency  $\nu$  of

$$\nu = 2 \frac{1}{\pi} \frac{d[\Delta\Phi(k)]}{dk} \dot{k} = \frac{d}{\pi} \dot{k} \quad (7)$$

and a finite bandwidth determined by  $\phi^{(O)}(k)$ .  $\nu$  plays the role of a carrier frequency:

$$I(t) \approx C_1 + C_2|E^{(O)}(\dot{k}t)|\cos[\phi^{(O)}(\dot{k}t) + 2\pi\nu t]. \quad (8)$$

To obtain  $P(z)$  by an inverse Fourier transform of  $I(t)$ , the carrier frequency  $\nu$  must exceed the bandwidth

$$\Delta\nu = \max \left[ \frac{1}{2\pi} \frac{d\phi^{(O)}(k)}{dk} \dot{k} \right]$$

of the scattered wave<sup>18</sup>; i.e., there is a minimal path difference  $d$  between the object and that reference beam that is approximately twice the optical thickness of the object.

### 4. Experimental Setup

Figure 2 shows a scheme of the experimental setup.

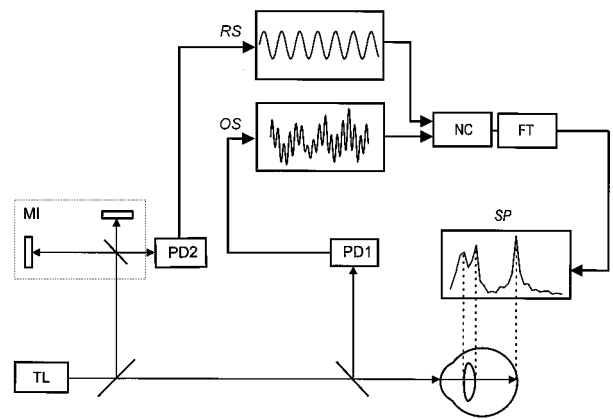


Fig. 2. Scheme of the wavelength tuning interferometer: OS, object signal; RS, reference signal; SP, scattering potential; MI, reference Michelson interferometer; FT, Fourier transform; NC, numerical correction; PD1, PD2, photodetectors; TL, tunable laser.

We used the dual-beam scheme, where the light beam reflected at the anterior corneal surface is used as the reference beam.<sup>30</sup> An external-cavity tunable laser diode is used as a light source (New Focus Model 6224). Its center wavelength is 780 nm with a mode-hop-free tuning range of  $\Delta\lambda \sim 9$  nm. Figure 3 shows the power spectrum.<sup>33</sup> This laser has two wavelength-tuning modes: A coarse tuning mode over the whole wavelength range of  $\sim 25$  nm accomplished with a low-speed picomotor with a maximum tuning rate of  $\sim 0.33$  nm/s. Fine tuning, the second mode, can be performed over a narrow bandwidth of  $\Delta\lambda \sim 0.18$  nm with a piezoelectric transducer. The maximum tuning rate is  $\sim 36$  nm/s in this case.

The photodetector, PD1, yields the electric object signal proportional to  $I(t)$ . The external Michelson interferometer, MI, with a known path-length difference is used to correct numerically the object signal obtained from PD1 to obtain constant  $\dot{k}$  and to calibrate the measured distances. Off-line fast Fourier transform on a PC is used to obtain the scattering potential of the object. Resolution  $\Delta z$  of WTI depends on the tuning range, see Eq. (3). The resolution obtained with a tuning range  $\Delta\lambda$  is of the same order as that of PCI employing a light source with

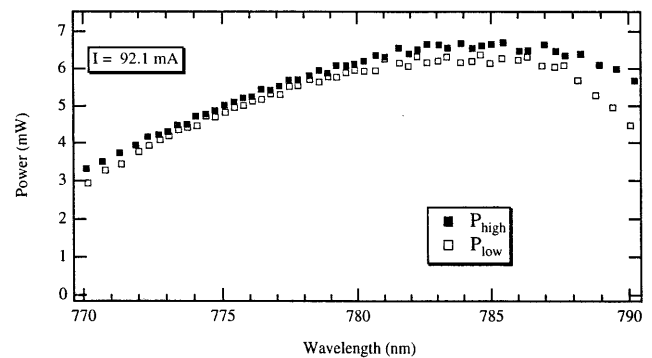


Fig. 3. Power spectrum of the tunable laser diode from New Focus Model 6224.<sup>33</sup>

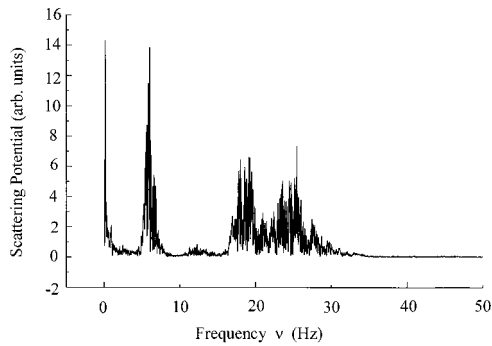


Fig. 4. WTI scan of an eye model obtained by Fourier transform of the photodetector signal  $I(k)$  by slow tuning over 9 nm. Frequency  $\nu$  is related by Eqs. (5) and (7) to optical distance. Note the broad peaks due to nonlinear  $\dot{k}$ .

spectral width  $\Delta\lambda$ ; i.e., when using the full tuning range, we have  $\Delta z \approx 11 \mu\text{m}$ , and when using the fine tuning range, we have  $\Delta z \approx 1.5 \text{ mm}$ .

Currently, because of the low tuning rate of the picomotor the whole mode-hop-free tuning range can be used only for *in vitro* measurements. For eye length measurements the expected signal frequency is of the order of 30 Hz. This is in the same range as the frequency of interference fringe oscillations due to fundus pulsations caused by the rhythmic filling of retinal blood vessels.<sup>34</sup> Since there is no possibility of separating these oscillations from those caused by WTI, this slow-speed tuning range can be used only for *in vitro* measurements.

The *in vivo* measurements were performed in healthy, volunteer subjects after full, informed consent was obtained. The whole *in vivo* measurement took  $\sim 10$  s. During this period the eye is illuminated with a laser light power of  $\sim 200 \mu\text{W}$  or an intensity of  $520 \mu\text{W}/\text{cm}^2$  (averaged over a 7-mm aperture). At a wavelength of  $\lambda = 780 \text{ nm}$  this is permitted for 10 min in the case of intrabeam viewing. Hence the safety limit is met.<sup>35</sup>

## 5. Results

An eye model, consisting of a lens and a transparent foil (simulating the retina) attached to a sheet of white paper (simulating the choroid), was used to perform measurements with the slow-speed wide-range tuning of the laser. The whole measurement, performed with the picomotor over a tuning range of 9 nm, took 28 s. Because of the use of the dual-beam scheme we obtain the autocorrelation function of the object structure. Hence the peaks in Fig. 4 (and Figs. 5 and 6) display distances between light remitting sites in the object. (If a true image structure is wanted, an external reference beam would have to be added.<sup>18</sup>) Because of nonlinearities of  $k(t)$  in wavelength tuning, the frequency peaks are distorted and broadened. In Fig. 5 the object scattering potential is plotted as a function of the optical distance to the anterior lens surface after numerical correction. From Fig. 5 the optical lens thickness and axial eye length are determined as  $9.165 \pm 0.005 \text{ mm}$  and  $38.275 \pm 0.035 \text{ mm}$ ,

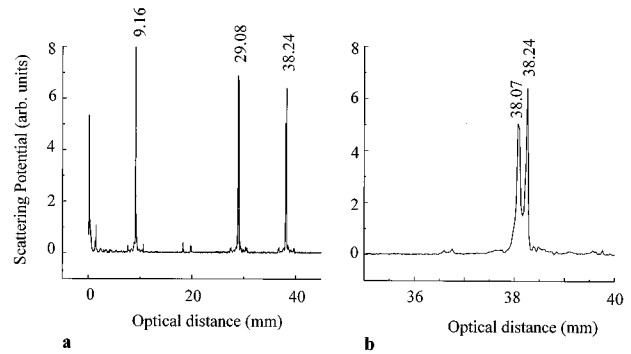


Fig. 5. (a) WTI scan of an eye model after numerical correction of the photodetector signal  $I(k)$  for constant  $\dot{k}$ . The signal peaks indicate the different optical distances measured: lens thickness, 9.16 mm; posterior lens surface–anterior foil surface, 29.08 mm; anterior lens surface–anterior foil surface, 38.24 mm. (b) Double peak caused by the 0.17-mm-thick foil.

respectively [mean values and standard deviations (SD) of four consecutive measurements]. The model eye was removed and realigned between the four consecutive measurements to evaluate the realignment error. For geometrical reasons this realignment error has larger effects on the larger axial eye length than on the shorter lens thickness, which explains the better SD in the latter case. Figure 5b shows the double peak caused by the transparent foil. The distance between these peaks indicates the foil thickness  $170 \mu\text{m} \pm 16 \mu\text{m}$ . The smaller peaks are caused by multiple reflections in the eye model and at surfaces in the instrument that are not perfectly antireflection coated.

*In vivo* measurements were performed in three healthy eyes with a high-speed tuning range of 0.15 nm. Because of this small tuning range the signal peaks in the frequency domain are broad, and consequently the measuring precision is rather poor. To demonstrate the simultaneous measurement of anterior segment and axial eye length, the measurement has to be performed along the optical axis of the eye rather than along the vision axis.<sup>36</sup> In each eye at least five measurements were performed. Figure 6 shows the result of an *in vivo* measurement of in-

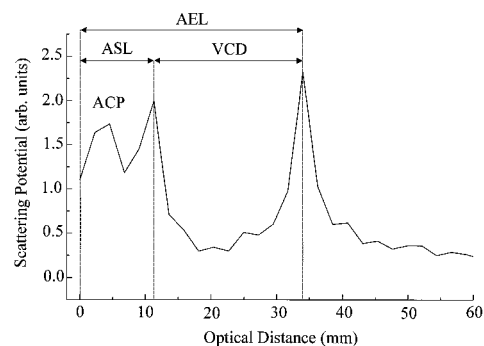


Fig. 6. WTI scan of a human eye *in vivo* obtained by high-speed piezotuning over 0.15 nm: ASL, anterior segment length; VCD, vitreous chamber depth; AEL, axial eye length; ACP, peak indicating anterior chamber depth (see text).

**Table 1. Measurement of Optical Intraocular Distances in Three Eyes *in Vivo*<sup>a</sup>**

Subject	WTI ASL (mm)	WTI AEL (mm)	PCI ASL (mm)	PCI AEL (mm)
CH	9.8	34.6	10.252	34.734
FL	10.5	35.3	10.610	35.289
WP	10.2	33.4	10.802	33.586

<sup>a</sup>Every eye was measured five times, and the results of WTI were compared with PCI: ASL, anterior segment length; AEL, axial eye length. The mean standard deviation of WTI was 0.82 mm, that of PCI  $\sim 3.3 \mu\text{m}$ .

traocular distances (on individual FL). Ten WTI scans recorded successively in the same eye were averaged to reduce the noise. Two signal peaks can clearly be identified. The peak at  $\sim 10.5$  mm is caused by light reflected at the posterior surface of the lens, and the peak at  $\sim 35.3$  mm indicates the position of the retina. This signal can be used to measure simultaneously three distances: anterior segment length (ASL) = 10.5 mm, vitreous chamber depth (VCD) = 24.8 mm, and axial eye length (AEL) = 35.3 mm. These optical distances have to be divided by the group refractive indices of the respective eye media to obtain geometric distances. The mean precision (SD) to which these peaks can be determined is 0.82-mm optical distance or 0.61-mm geometric distance. The broad signal peak labeled ACP might indicate the anterior chamber depth. However, intensity oscillations of the laser beam during piezotuning produce a signal peak at the corresponding frequency, which prevents an unambiguous identification of the anterior lens surface peak.

The results obtained in the measurements of three healthy eyes were compared with results obtained by PCI (cf. Table 1). PCI data were measured with an interferometric setup, which is described in detail elsewhere.<sup>37</sup> They are equal within the standard deviation of WTI.

## 6. Conclusion

The application of WTI to measure intraocular distances simultaneously has been demonstrated. This technique does not need a moving reference mirror such as conventional low-coherence interferometry ranging. High resolution has been obtained in a model eye by scanning the wavelength over the entire mode-hop-free range of 9 nm. The simultaneous *in vivo* measurement of three intraocular distances has been demonstrated although with low resolution. The acquisition time of a single WTI scan was 5 ms. The resolution of *in vivo* WTI measurements might be improved by using a distributed Bragg reflector tunable laser diode. In this case, the tuning is accomplished by changing the drive currents of the different sections of the diode rather than by mechanical elements as with external cavity diodes. This enables a tuning over of 1–2 nm within milliseconds. This tuning range is not sufficient for high-resolution OCT, but it is of the same order as the spectral width

of the laser diode we used recently to measure the axial length of cataract eyes.<sup>38</sup> Therefore this tuning range should be sufficient to measure intraocular distances with a precision of  $\sim 30 \mu\text{m}$ . This would be  $\sim 5$  times better than the precision obtained with currently used ultrasound instruments. The main advantage of such a medium-precision biometry instrument would be a compact optical design and a millisecond measuring time. The location of intraocular interfaces along the whole eye length could be obtained in milliseconds compared with a few seconds of the currently used PCI instruments.

The authors thank W. Drexler for supplying the PCI data and H. Sattmann for technical assistance. The authors are obliged to a referee who drew their attention to Refs. 20–23. Financial support from the Austrian Fonds zur Förderung der wissenschaftlichen Forschung (FWF grants P9781-MED and P10316-MED) is acknowledged.

## References

1. A. F. Fercher, K. Mengedoht, and W. Werner, "Eye length measurement by interferometry with partially coherent light," *Opt. Lett.* **13**, 186–188 (1988).
2. C. K. Hitzenberger, "Optical measurement of the axial eye length by laser Doppler interferometry," *Inv. Ophthalmol. Visual Sci.* **32**, 616–624 (1991).
3. D. Huang, J. Wang, C. P. Lin, C. A. Puliafito, and J. G. Fujimoto, "Micron-resolution ranging of cornea anterior chamber by optical reflectometry," *Lasers Surg. Med.* **11**, 419–425 (1991).
4. D. Huang, E. A. Swanson, C. P. Lin, J. S. Schuman, W. G. Stinson, W. Chang, M. R. Hee, T. Flotte, K. Gregory, C. A. Puliafito, and J. G. Fujimoto, "Optical coherence tomography," *Science* **254**, 1178–1181 (1991).
5. E. A. Swanson, J. A. Izatt, M. R. Hee, D. Huang, C. P. Lin, J. S. Schuman, C. A. Puliafito, and J. G. Fujimoto, "In vivo retinal imaging using optical coherence tomography," *Opt. Lett.* **18**, 1864–1866 (1993).
6. A. F. Fercher, C. K. Hitzenberger, W. Drexler, G. Kamp, and H. Sattmann, "In vivo optical coherence tomography," *Am. J. Ophthalmol.* **116**, 113–114 (1993).
7. A. F. Fercher, C. Hitzenberger, and M. Juchem, "Measurement of intraocular optical distances using partially coherent laser light," *J. Mod. Opt.* **38**, 1327–1333 (1991).
8. D. Roschdestwensky, "Anomale Dispersion im Natriumdampf," *Ann. Phys.* **39**, 307–345 (1912).
9. H. Kopfermann and R. Ladenburg, "Untersuchungen über die anomale Dispersion angeregter Gase," *Z. Phys.* **48**, 15–61 (1928).
10. P. D. Fochs, "A method for determining concurrently the thickness and refractive index of a thin-film lamina," *J. Opt. Soc. Am.* **40**, 623 (1950).
11. M. A. Jeppesen and A. M. Taylor, "Thickness and refractive index measurement of a lamina with a Michelson interferometer," *J. Opt. Soc. Am.* **56**, 451–455 (1966).
12. K.-P. Koch, M. Maechler, and F. Glueck, "Application of diode array spectrometers in microscope photometry," *Rev. Sci. Instrum.* **56**, 2243–2247 (1985).
13. L. Montgomery Smith and C. C. Dobson, "Absolute displacement measurements using modulation of the spectrum of white light in a Michelson interferometer," *Appl. Opt.* **28**, 3339–3342 (1989).
14. A. P. Kovacs, K. Osvay, and Zs. Bor, "Group-delay measurement on laser mirrors by spectrally resolved white-light interferometry," *Opt. Lett.* **20**, 788–790 (1995).

15. T. Dresel, G. Häusler, and H. Venzke, "Three-dimensional sensing of rough surfaces by coherence radar," *Appl. Opt.* **31**, 919–925 (1992).
16. A. F. Fercher, W. Drexler, C. K. Hitzenberger, and G. Kamp, "Measurement of ocular distances by optical spectrum modulation," in *Microscopy, Holography, and Interferometry in Biomedicine*, A. F. Fercher, A. Lewis, H. Podbielska, H. Schneckenburger, and T. Wilson, eds., *Proc. SPIE* **2083**, 263–267 (1993).
17. G. Häusler, J. Herrmann, and J. Neumann, "Verfahren zur Ermittlung der Entfernung und Streuintensität von streuenden Punkten," Patent Application DE 43 09 056 A1 (22 September 1994).
18. A. F. Fercher, C. K. Hitzenberger, G. Kamp, and S. Y. El-Zaiat, "Measurement of intraocular distances by backscattering spectral interferometry," *Opt. Commun.* **117**, 43–48 (1995).
19. A. Sekine, I. Minegishi, and H. Koizumi, "Axial eye-length measurement by wavelength-shift interferometry," *J. Opt. Soc. Am. A* **10**, 1651–1655 (1993).
20. A. Hymans and M. A. Lait, "Analysis of a frequency-modulated continuous-wave ranging system," *Proc. Inst. Electron. Eng.* **107**, 365–372 (1960).
21. R. I. MacDonald, "Frequency domain optical reflector," *Appl. Opt.* **20**, 1840–1844 (1981).
22. W. Eickhoff and R. Ulrich, "Optical frequency domain reflectometry in single-mode fiber," *Appl. Phys. Lett.* **39**, 693–695 (1981).
23. K. Takada and H. Yamada, "Narrow-band light source with acousto-optic tunable filter for optical low-coherence reflectometry," *IEEE Photon. Tech. Lett.* **8**, 658–660 (1996).
24. T. L. Koch and U. Koren, "Semiconductor lasers for coherent optical fiber communications," *J. Lightwave Technol.* **8**, 274–293 (1990).
25. E. Wolf, "Three-dimensional structure determination of semi-transparent objects from holographic data," *Opt. Commun.* **1**, 153–156 (1969).
26. A. C. Kak and M. Slaney, *Principles of Computerized Tomographic Imaging* (IEEE, New York, 1988).
27. A. F. Fercher, H. Bartelt, H. Becker, and E. Wiltchko, "Image formation by inversion of scattered field data: experiments and computational simulation," *Appl. Opt.* **18**, 2427–2439 (1979).
28. R. Dändliker and K. Weiss, "Reconstruction of the three-dimensional refractive index from scattered waves," *Opt. Commun.* **1**, 323–328 (1970).
29. Y. Pan, R. Birngruber, J. Rosperich, and R. Engelhardt, "Low-coherence optical tomography in turbid tissue: theoretical analysis," *Appl. Opt.* **34**, 6564–6574 (1995).
30. A. F. Fercher, "Optical coherence tomography," *J. Biomed. Opt.* **1**, 157–173 (1996).
31. A. F. Fercher, W. Drexler, and C. K. Hitzenberger, "OCT techniques," in *Lasers in Ophthalmology IV*, R. Birngruber, A. F. Fercher, and P. Sourdille, eds., *Proc. SPIE* **2930**, 164–174 (1996).
32. R. Bracewell, *The Fourier Transform and Its Applications* (McGraw-Hill, New York, 1965).
33. *Acceptance Test Data Sheet* (New Focus Inc., Santa Clara, Calif., 1996).
34. L. Schmetterer, F. Lexer, C. J. Unfried, H. Sattmann, and A. F. Fercher, "Topical measurement of fundus pulsations," *Opt. Eng.* **34**, 711–716 (1995).
35. American National Standards Institute, *Safe Use of Lasers*, ANSI Z 136.1 (American National Standards Institute, New York, 1986).
36. A. Baumgartner, C. K. Hitzenberger, W. Drexler, H. Sattmann, and A. F. Fercher, "Measurement of the anterior structures of the human eye by partial coherence interferometry," in *Lasers in Ophthalmology II*, R. Brancato, A. F. Fercher, A. S. Melamed, and P. O. Rol, eds., *Proc. SPIE* **2330**, 146–151 (1995).
37. W. Drexler, C. K. Hitzenberger, H. Sattmann, and A. F. Fercher, "Measurement of the thickness of fundus layers by partial coherence tomography," *Opt. Eng.* **34**, 701–710 (1995).
38. C. K. Hitzenberger, W. Drexler, C. Dolezal, F. Skorpik, M. Juchem, A. F. Fercher, and H. D. Gnad, "Measurement of the axial length of cataract eyes by laser Doppler interferometry," *Inv. Ophthalmol. Visual Sci.* **34**, 1886–1893 (1993).